Kupffer Cell Suppression of CD8+ T Cells in Human Hepatocellular Carcinoma Is Mediated by B7-H1/Programmed Death-1 Interactions

Ke Wu,[1] Ilona Kryczek,[1] Lieping Chen,[2] Weiping Zou,[1] and Theodore H. Welling[1]

[1]Department of Surgery, University of Michigan, Ann Arbor, Michigan and [2]Department of Oncology, Sidney Kimmel Comprehensive Cancer Center, The Johns Hopkins University, Baltimore, Maryland

Abstract

B7-H1 is a recently identified B7 family member that, along with one of its receptors, programmed death-1 (PD-1), has been involved in multiple immunopathologic scenarios. However, the nature of B7-H1 and PD-1 in human hepatocellular carcinoma (HCC) remains poorly defined. We investigated the expression and functional relevance of this pathway in patients with HCC. We showed that B7-H1 expression on Kupffer cells (KC) was increased in tumor tissues compared with surrounding nontumor liver tissues in patients with HCC and this correlated with poorer survival. Coculture of HCC cells with monocytes showed that tumor-associated interleukin-10 contributed to the induction of B7-H1 in the HCC environment. We further observed that the levels of PD-1$^+$CD8$^+$ T cells were higher in tumor tissues than in nontumor tissues. B7-H1$^+$ KCs and PD-1$^+$ T cells were colocalized in the HCC stroma. PD-1$^+$CD8$^+$ T cells had decreased proliferative ability and effector function as shown by reduced granule and cytokine expression compared with PD-1$^-$ T cells. Importantly, blocking KC B7-H1 interaction with PD-1$^+$CD8$^+$ cells using neutralizing antibodies recovered effector T-cell function. Our data indicate that the B7-H1/PD-1 axis contributes to immune suppression in human HCC, with blockade of this pathway carrying important therapeutic implications. [Cancer Res 2009;69(20):8067–75]

Introduction

Hepatocellular carcinoma (HCC) is the most common primary hepatic malignancy and is the second most common cause of cancer-related deaths in the world. Although resection and transplantation are possible therapeutic options, 5-year recurrence rates following resection can exceed 50% (1). Several variables affect the risk of recurrence following resection, including tumor size, tumor number, and vascular invasion. However, the role of tumor immunity is increasingly being recognized as being important to controlling tumor progression or recurrence in cases of breast, ovarian, and pancreatic cancers along with many others (2). Recently, HCC recurrence and stage is independently predicted by the degree of CD8$^+$ tumor-infiltrating T cells (3). CD8$^+$ CTLs are the major effectors against tumor cells (4). However, the progression of HCC and other tumors despite the presence of infiltrating CD8$^+$ T cells stresses the pathologic significance of the regulatory mechanisms within the tumor microenvironment. Recent evidence suggests that CD8$^+$ T cells may become dysfunctional or functionally exhausted within the tumor microenvironment (5).

Programmed death-1 (PD-1; CD279) may have an important role in the exhaustion of CD8$^+$ T cells in infectious diseases (6, 7). Functionally exhausted CD8$^+$ T cells express high levels of PD-1. PD-1 has two ligands with distinct expression patterns: B7-H1 [programmed death ligand 1 (PD-L1); CD274] and B7-DC (PD-L2; CD273). B7-H1 is expressed on resting T cells, B cells, dendritic cells, and macrophages and is further up-regulated on activation (8). B7-H1, which acts as an antiapoptotic receptor, is also expressed on some tumor cells (9). In contrast, B7-DC is expressed only on DC and macrophages following induction (10). Ligation of PD-1 by B7-H1 transduces a negative signal when transmitted simultaneously with T-cell receptor (TCR) signaling. This negative regulatory function is accomplished through the cytoplasmic domain of the molecule, which recruits intracellular phosphatases SHP-1 and SHP-2 (6). The recruitment of these phosphatases to the membrane leads to the dephosphorylation of several key signaling intermediates and thus the attenuation of TCR-mediated signals and T-cell activation. It has been shown that B7-H1/PD-1 interactions contribute to the suppression of antiviral immunity in liver or antitumor immunity (11–16). However, little is known about the functional relevance and mechanism of B7-H1 and PD-1 in human HCC.

The liver is an immunologically privileged site as studied in oral tolerance and transplantation models (17). Tolerogenic or suppressive antigen-presenting cells (APC), numerous in liver tissue, are thought to control tolerogenic phenotypes. Recently, B7-H1 was shown to be expressed on hepatocytes and liver residential APCs, contributing to deletion of intrahepatic T cells, preventing hepatic autoimmunity, and suppressing antiviral immune responses in animal models (18, 19). Given the relative paucity of data on the HCC microenvironment, we studied tumor tissues and surrounding nontumor liver tissues in HCC patients undergoing surgical resection and investigated the expression and functional relevance of B7-H1 and PD-1 in the human HCC microenvironment. Evidence is provided that Kupffer cells (KC) primarily express B7-H1 in human HCC and mediate decreased effector function via interaction with PD-1 on effector T cells. Furthermore, this suppression seems to be reversible following disruption of these interactions, carrying potential immunotherapeutic implications.

Materials and Methods

Human tissues. For functional analysis, fresh HCC tissues and surrounding nontumor liver tissues were obtained from HCC patients undergoing surgical resection. The surrounding liver tissues from benign liver tumors served as normal liver controls. For survival analysis, 71 patients with HCC following surgical resection at the Sun Yat-Sen University Cancer Center (Guang Zhou, China) from July 2000 to December

Note: Supplementary data for this article are available at Cancer Research Online (http://cancerres.aacrjournals.org/).

Requests for reprints: Theodore H. Welling, Department of Surgery, University of Michigan, 1150 West Medical Center Drive, Ann Arbor, MI 48109. Phone: 734-936-9623; Fax: 734-763-3187; E-mail: twelling@umich.edu.

©2009 American Association for Cancer Research.

doi:10.1158/0008-5472.CAN-09-0901

Downloaded from http://aacrjournals.org/cancerres/article-pdf/69/20/8067/2615403/8067.pdf by guest on 01 December 2023

2002 were studied. These tissues were analyzed for tumor tissue B7-H1 expression by immunohistochemistry. The clinical characteristics of all patients are summarized in Table 1. All patients gave written informed consent. The study was approved by the local institutional review boards.

Cell isolation. Cells were obtained from fresh HCC or surrounding liver tissues. The tissues were minced and digested with 50 mL HBSS (Life Technologies) containing 40 mg collagenase, 4 mg DNase I, and 100 units hyaluronidase (Sigma) for 2 h at room temperature. Tumor-infiltrating leukocytes (TIL) or non-TILs were isolated by Ficoll gradient centrifugation and analyzed by LSR II (BD Biosciences). $CD8^+$ T cells and $CD14^+$ tumor-associated KCs were isolated and purified with paramagnetic beads (StemCell Technology). $Lin^-CD45^-CD14^-$ HCC tumor cells were sorted with FACSAria using DiVa software (Becton Dickinson Immunocytometry Systems).

Cell culture. $CD8^+$ T cells (5×10^5/mL) were added to 96-well round-bottomed cluster plates and stimulated with anti-human CD3 (2.5 μg/mL, clone UCHT1; BD Biosciences) and anti-human CD28 (1.2 μg/mL, clone CD28.2; BD Biosciences) in the presence of HCC-associated KCs (1×10^5/mL) from the same tissue or $CD14^+$ cells from the blood of healthy donors for 5 d. Neutralizing monoclonal antibody against human PD-1 (clone M3, 5 μg/mL) and B7-H1 (clone 5H1, 5 μg/mL; ref. 17) or isotype controls were used in coculture as indicated. After coculture, cells were subjected to fluorescence-activated cell sorting (FACS) analysis or proliferation assay.

Flow cytometry. Anti-human CD3, CD4, CD8, CD11c, CD14, CD45, CD123, HLA-DR, B7-H1, PD-1, Foxp3, granzyme B, perforin, IFNγ, and tumor necrosis factor α (TNFα) antibodies (BD Biosciences) were used in FACS and compared with isotype antibody controls as appropriate. Anti-human Ki67 (BD Biosciences) staining was used to identify proliferating cells. For intracellular cytokine staining, cells were exposed for 4 h with phorbol 12-myristate 13-acetate (PMA; 50 ng/mL; Sigma), ionomycin (500 ng/mL; Sigma), GolgiStop (1 μL/1.5 mL; BD Biosciences), and GolgiPlug (1 μL/mL; BD Biosciences) as previously described (20) followed by surface and intracellular staining of various cytokines according to the manufacturer's instructions (BD Biosciences).

Immunohistochemistry. Fluorescence immunohistochemistry was performed on 8-μm cytosections of tissues. Briefly, tissues were stained as indicated with primary antibodies, including mouse anti-human B7-H1 (clone MIH1, IgG1, 1:100; BD Biosciences), mouse anti-human CD68 (clone Y1/82A, IgG2b, 1:100; BD Biosciences), mouse anti-human PD-1 (clone NAT, IgG1, 1:200; Abcam), goat anti-human PD-1 (IgG, 1:100; R&D Systems, Inc.), and rat anti-human CD8 (clone YTC182.20, IgG2b, 1:200; Abcam). Secondary antibodies were Alexa Fluor 568–conjugated goat anti-mouse IgG1, Alexa Fluor 488–conjugated goat anti-mouse IgG2b, Alexa Fluor 488–conjugated donkey anti-goat IgG, Alexa Fluor 568–conjugated goat anti-mouse IgG1, or Alexa Fluor 488–conjugated goat anti-rat IgG (all 2 μg/mL; Molecular Probes). 4′,6-Diamidino-2-phenylindole (DAPI; Invitrogen) was used for nuclear staining. Fluorescent expression was evaluated with the Leica DM 5000B fluorescence microscope and compared with antibody isotype controls. Positive cells were quantified by ImagePro Plus software (Media Cybernetics) and expressed as the mean number of positive cells ± SE in 10 high-powered fields. For survival analysis, experiments were performed by two independent observers who were blinded to the clinical outcome. At low power field (×100), the tissue sections were screened using a Leica DM IRB inverted research microscope (Leica Microsystems), and the five most representative fields were selected. Thereafter, to evaluate the density of $B7\text{-}H1^+$ cells, the respective areas of tumor tissue were measured at ×400 magnification, and the nucleated cells positive for B7-H1 in each area were counted and expressed as number of cells per field.

Transwell experiments. Hep G2 cells were obtained from the American Type Culture Collection. The cells were grown in DMEM. Six-well Transwell chambers with a 0.4-μm porous membrane (Corning Costar) were used. Briefly, primary HCC tumor cells or Hep G2 cells (2×10^6/mL), where indicated, were added in the upper chamber and $CD14^+$ cells (0.5×10^6/mL) from blood of healthy donors were plated to the lower chambers. Recombinant human interleukin-10 (IL-10; 10 ng/mL; R&D Systems) or monoclonal antibody against human IL-10 (500 ng/mL; R&D Systems) were added to select wells in the upper chamber. After 48 h, $CD14^+$ cells were harvested and B7-H1 expression was determined by FACS. Where indicated, supernatants from Transwell experiments and cultured cells were checked by human IL-10 ELISA kit (R&D Systems).

Western blot analysis and real-time reverse transcription-PCR. Single-cell suspensions from HCC tumor tissues and surrounding liver tissues were used for Western blot analysis and real-time reverse transcription-PCR (RT-PCR). Briefly, for Western blot analysis, whole-cell lysates were prepared by incubating cells in ice-cold lysis buffer [20 mmol/L Tris (pH 7.8), 2 mmol/L EDTA, 50 mmol/L NaF, 1% Triton X-100, 5 μg/mL leupeptin, 5 μg/mL pepstatin, 0.5 mmol/L phenylmethylsulfonyl fluoride]. The lysates were then centrifuged at 14,000 × *g* for 15 min at 4°C and assayed for protein with the Bio-Rad protein assay reagent. Equal amounts of protein were resolved by SDS-PAGE and transferred to nitrocellulose membranes. The following antibodies for Western blots were used: mouse anti-human IL-10 (clone 25209, IgG2b, 1:1,000; R&D Systems) and mouse anti-human β-actin (clone AC-15, IgG1, 1:2,000; Sigma). Images were visualized with an enhanced chemiluminescence detection system (Amersham Biosciences; ref. 21). For RT-PCR, total RNA from tumor tissues and liver tissue as indicated was isolated using RNeasy kits (Qiagen). cDNA synthesis was performed using SuperScript One-Cycle cDNA kit (Invitrogen). The cDNA served as a template in real-time PCR using Fast SYBR Green Master kit (Applied Biosystems). The following primers for RT-PCR were used: human IL-10 primers, 5′-CATTCTTCACCTGCTCCAC-G-3′ (sense) and 5′-AACCTGCCTAACATGCTTCG-3′ (antisense; ref. 22); human glyceraldehyde-3-phosphate dehydrogenase (GAPDH) primers, 5′-CTGCCCCCTCTGCTGATG-3′ (sense) and 5′-TCCACGATACCAAAGTTG-TCATG-3′ (antisense; ref. 23). All reactions were performed in triplicate. IL-10 mRNA expression of different group specimens was normalized to GAPDH. Relative IL-10 mRNA levels are presented as unit values of $2^{-\Delta Ct} = 2^{-[Ct\ (GAPDH)\ -\ Ct\ (IL\text{-}10)]}$, where C_t is the threshold cycle value defined as the fractional cycle number at which the target fluorescent signal passes a fixed threshold above baseline.

Proliferation assay. After 5 d of coculture, T cells were pulsed with [^{3}H]thymidine for the final 16 h of incubation. Incorporation of [^{3}H]thymidine was measured with a microbeta liquid scintillation counter (Perkin-Elmer).

IFNγ enzyme-linked immunospot assay. MultiScreen filtration plates (96-wells per plate; Millipore) were coated with 100 μL/well of 4 μg/mL purified anti-human IFNγ antibody (clone NIB42; BD Pharmingen) overnight at 4°C and then incubated for 90 min at room temperature with 150 μL/well of 1% bovine serum albumin (Sigma) in PBS. $CD8^+$ cells (1×10^5/100 μL/well) and $CD14^+$ cells (5×10^4/100 μL/well) from tumor tissues were placed into 96-well round-bottomed cluster plates in the presence of anti-human CD28 (1.2 μg/mL, clone CD28.2; BD Biosciences) for 5 d at 37°C, 5% CO_2 in presence or absence of anti-human B7-H1 (clone 5H1, 5 μg/mL) or anti-human PD-1 (clone M3, 5 μg/mL) antibody. Then, all the cells were transferred to MultiScreen filtration plates and incubated for 48 h in the presence of HCC tumor cells lysate (from 1×10^4 per well) at 37°C, 5% CO_2. PMA (1 ng/mL)–treated and ionomycin (0.5 μg/mL)–treated $CD8^+$ effector cells served as a positive control (~100 spots per well; data not shown). Plates were washed and incubated overnight at 4°C with 100 μL/well of 4 μg/mL of biotinylated rat anti-human IFNγ antibody (clone 4S.B3; BD Pharmingen) followed by a 90-min incubation with 100 μL/well anti-biotin alkaline phosphatase (Vector Laboratories, Inc.) diluted 1:1,000. Spots were visualized with 5-bromo-4-chloro-3-indolyl phosphate/nitroblue tetrazolium alkaline phosphatase substrate and counted using the ImmunoSpot analyzer (Cellular Technology Ltd.).

Statistical analysis. Data are presented as the mean ± SE. Significant differences between groups were analyzed using Wilcoxon matched-pairs rank test for nonparametric data or one-way ANOVA test, where appropriate. *P* values of <0.05 were considered statistically significant. For survival analysis, survival curves were compared by the Kaplan-Meier method and the log-rank test, and survival was measured in months from resection to the last review. All analyses were done using Statistical Package for the Social Sciences v12.0 software.

Downloaded from http://aacrjournals.org/cancerres/article-pdf/69/20/8067/2615403/8067.pdf by guest on 01 December 2023

Table 1. Clinical characteristics of HCC patients

Variables	Results
No. patients	71
Age, y (median, range)	48, 23–75
Gender (male/female)	65/6 (92/8)
HBsAg (negative/positive)	8/63 (11/89)
Cirrhosis (absent/present)	16/55 (23/77)
ALT, units/L (median, range)	40, 11–179
AFP, ng/mL (≤25/>25)	27/44 (38/62)
Tumor size, cm (≤5/>5)	36/35 (51/49)
Tumor multiplicity (solitary/multiple)	63/8 (89/11)
Vascular invasion (absent/present)	69/2 (91/9)
Intrahepatic metastasis (no/yes)	68/3 (96/4)
TNM stage (I + II/III + IV)	57/14 (80/20)
Tumor differentiation (I + II/III + IV)	58/13 (82/18)
Fibrous capsule (absent/present)	13/58 (18/82)
B7-H1$^+$ cells (median, range)	94, 16–227

NOTE: Data in parentheses are percentages.
Abbreviations: HBsAg, hepatitis B surface antigen; AFP, α-fetoprotein; ALT, alanine aminotransferase; TNM, tumor-node-metastasis.

Results

B7-H1 expression on APC subsets in human HCC. We analyzed the prevalence and phenotype of APC subsets within paired tumor tissues and surrounding liver tissues in patients with HCC (n = 20). The major human APC subsets, including HLA-DR$^+$CD14$^+$ KCs, Lin$^-$HLA-DR$^+$CD4$^+$CD11c$^+$ myeloid dendritic cells (mDC), and Lin$^-$HLA-DR$^+$CD4$^+$CD11c$^-$CD123$^+$ plasmacytoid dendritic cells (pDC), were found in both tumor tissues and surrounding nontumor liver tissues. The proportion of pDCs (1 ± 0.5%), mDCs (5 ± 2%), and KCs (20 ± 5%) in CD45$^+$HLA-DR$^+$ leukocytes was comparable between tumor tissues and nontumor tissues (Fig. 1*A*). We next examined the expression of B7-H1 on these APC subsets. mDCs and pDCs expressed negligible levels of B7-H1 (Supplementary Fig. S1). Similar to our previous observation on ovarian cancer–associated macrophages (12), KCs were the predominant B7-H1$^+$ population in HCC microenvironment. The percentage of B7-H1$^+$ KCs was higher in tumor tissues than surrounding liver tissues [17.6 ± 4.1% versus 7 ± 2.7%, n = 15, P < 0.05, both by percentage of cells and mean fluorescence intensity (MFI)] when compared with antibody isotype controls (Fig. 1*B*; Supplementary Fig. S1). Further, the levels of B7-H1 expression on tumor-associated KCs were significantly higher than that on other APC subsets in different compartments (Supplementary Fig. S1). Using immune fluorescence staining, we confirmed that CD68$^+$ KCs expressed more B7-H1 in HCC tumor tissues (Fig. 1*C, a*) than in surrounding nontumor (Fig. 1*C, b*) and normal liver tissues (Fig. 1*C, c*). Cells were negative for staining with isotype control antibodies (Fig. 1*C, d*).

To evaluate whether B7-H1 expression is a prognostic factor for survival after HCC tumor resection, 71 patients were divided into a low B7-H1–expressing and a high B7-H1–expressing group by using the median value of B7-H1$^+$ cell density in tumor tissues on immunohistochemistry. Overall, the high B7-H1–expressing group experienced worse survival when compared with the lower B7-H1–expressing group following log-rank analysis (Fig. 1*D*). The data indicate that high levels of B7-H1 are expressed in the HCC microenvironment, which correlated with worse prognosis, and that B7-H1 is primarily expressed on KCs in HCC tumor tissues.

Tumor-associated IL-10 induced B7-H1 expression on KCs. Our previous work in human ovarian carcinoma indicated that tumor-associated IL-10 can up-regulate B7-H1 expression (15). Therefore, we examined the potential factors in the HCC microenvironment contributing to KC B7-H1 up-regulation. We cocultured blood CD14$^+$ monocytes from healthy donors with primary HCC tumor cells or Hep G2 cells. Monocyte B7-H1 expression was significantly increased in the coculture with HCC tumor cells or Hep G2 cells (Fig. 2*A*). Increased levels of IL-10 were also detected in the cocultures (Fig. 2*B*). Additionally, both mRNA and protein expression of IL-10 were increased in primary HCC tumor tissues compared with surrounding liver tissues (Fig. 2*C* and *D*). The addition of recombinant IL-10 moderately induced B7-H1 expression on monocytes (Fig. 2*A*), whereas neutralizing antibody against IL-10 significantly blocked monocyte B7-H1 expression induced in coculture. These results suggest that HCC-associated IL-10 production may contribute to increased KC B7-H1 expression in the HCC microenvironment.

PD-1 expression on T-cell subsets in human HCC. We further analyzed the prevalence and phenotype of T-cell subsets within paired tumor tissues and surrounding liver tissues in patients with HCC (n = 20). We observed significant and comparable CD4$^+$ and CD8$^+$ T-cell infiltration in tumor tissues and surrounding liver tissues (Fig. 3*A, top*). Because PD-1 is the coinhibitory signal receptor for B7-H1 and CD8$^+$ cytotoxic T cells are the main effector in antitumor immune responses (4), we examined the phenotype of PD-1$^+$CD8$^+$ T cells. Both in HCC tumor tissues and surrounding liver tissue, <5% of CD8$^+$ T cells are CD45RA$^+$ or CD62L$^+$ (Fig. 3*A, bottom*). The percentage of PD-1$^+$CD8$^+$ T cells was higher (63.0 ± 20.3%) in tumor tissues than that in surrounding tissues (11.5 ± 6.0%, P < 0.05; Fig. 3*B* and *C*). The expression of PD-1 on CD8$^+$ T cells in HCC tumor tissue (Fig. 3*D, a*) was confirmed by immunohistochemistry and was much higher than in surrounding nontumor (Fig. 3*D, b*) and normal liver tissues (Fig. 3*D, c*). Cells were negative for staining with isotype control antibodies (Fig. 3*D, d*). PD-1$^+$ cells were also found to be localized primarily to the HCC stroma (Supplementary Fig. S2). CD80, another reported receptor for B7-H1 (24), was not detected on CD8$^+$ cells nor was B7-DC, another ligand for PD-1 (10), detected on KC or DC (data not shown). These results indicate that most of CD8$^+$ T cells within human HCC are effector phenotype, with a greater percentage of these expressing PD-1 in the tumor microenvironment.

Functional characteristics of tumor-associated PD-1$^+$CD8$^+$ T cells in human HCC. Given the high levels of PD-1 expression on CD8$^+$ T cells in HCC, effector T cells might be functionally exhausted. We examined the functional characteristics of tumor-associated PD-1$^+$CD8$^+$ T cells in human HCC. We initially compared the *in vivo* proliferation status of CD8$^+$ T cells in tumor tissues versus surrounding liver tissues and of PD-1$^+$CD8$^+$ T cells versus PD-1$^-$CD8$^+$ T cells in human HCC using Ki67, a proliferative marker for cells in mitosis. The levels of Ki67$^+$CD8$^+$ T cells were lower in tumor tissues than surrounding tissues (Fig. 4*A*). Furthermore, PD-1$^+$CD8$^+$ T cells were less proliferative than PD-1$^-$CD8$^+$ T cells in patients with HCC (Fig. 4*B*). PD-1 has previously been shown in animal models to negatively regulate CD8$^+$ T-cell effector function (19, 20). We further examined the functional markers of effector T cells, including cytokine profile and cytotoxic

Downloaded from http://aacrjournals.org/cancerres/article-pdf/69/20/8067/2615403/8067.pdf by guest on 01 December 2023

enzymes. PD-1$^+$CD8$^+$ T cells in tumors exhibited markedly diminished expression of perforin and granzyme B (Fig. 4*C* and *D*). Furthermore, the percentage of TNFα$^+$ and IFNγ$^+$ T cells was significantly reduced in PD-1$^+$CD8$^+$ T cells than in PD-1$^-$CD8$^+$ T cells (Fig. 4*C* and *D*). These results indicate that PD-1$^+$CD8$^+$ T cells in the HCC microenvironment have impaired effector function when compared with PD-1$^-$CD8$^+$ T cells.

B7-H1/PD-1 interactions mediate impaired effector T-cell function in human HCC. To identify whether B7-H1$^+$ KCs interact with PD-1$^+$CD8$^+$ T cells in HCC, human HCC tumor specimens were further analyzed by immunohistochemistry to determine their physical localization. A significant infiltration of B7-H1$^+$ and PD-1$^+$ cells was detected in the peritumor stroma when compared with the tumor nests (Supplementary Fig. S2). In addition, B7-H1$^+$ and PD-1$^+$ cells seemed to be in close contact with each other, providing the possibility for direct interactions between these cells (Fig. 5*A*). To evaluate whether disruption of the B7-H1/PD-1 interaction would restore effector function to CD8$^+$ T cells, CD8$^+$ T cells and KCs were sorted from HCC tumor tissues and placed into coculture. Tumor-derived KC caused no increase in CD8$^+$ proliferation or cytokine proliferation (data not shown). However, blockade of B7-H1 or PD-1 with specific monoclonal antibodies resulted in enhanced T-cell proliferation as shown by [^{3}H]thymidine incorporation (Fig. 5*B*) and Ki67 expression (Fig. 5*C*), T-cell effector cytokine expression, granzyme B expression, and perforin expression compared with no treatment isotype control group (Fig. 5*C*). To evaluate whether B7-H1/PD-1 interactions affect tumor antigen-specific responses, we further performed HCC-specific IFNγ enzyme-linked immunospot (ELISPOT) analysis using HCC-derived KCs loaded with HCC lysates to stimulate autologous HCC CD8$^+$ T cells. Blocking B7-H1 or PD-1 using monoclonal antibodies increased the antigen-specific IFNγ-secreting spots (Fig. 5*D*), suggesting that B7-H1$^+$ KCs interact with PD-1$^+$CD8$^+$ T cells and contribute to dysfunction of effector T cells in HCC.

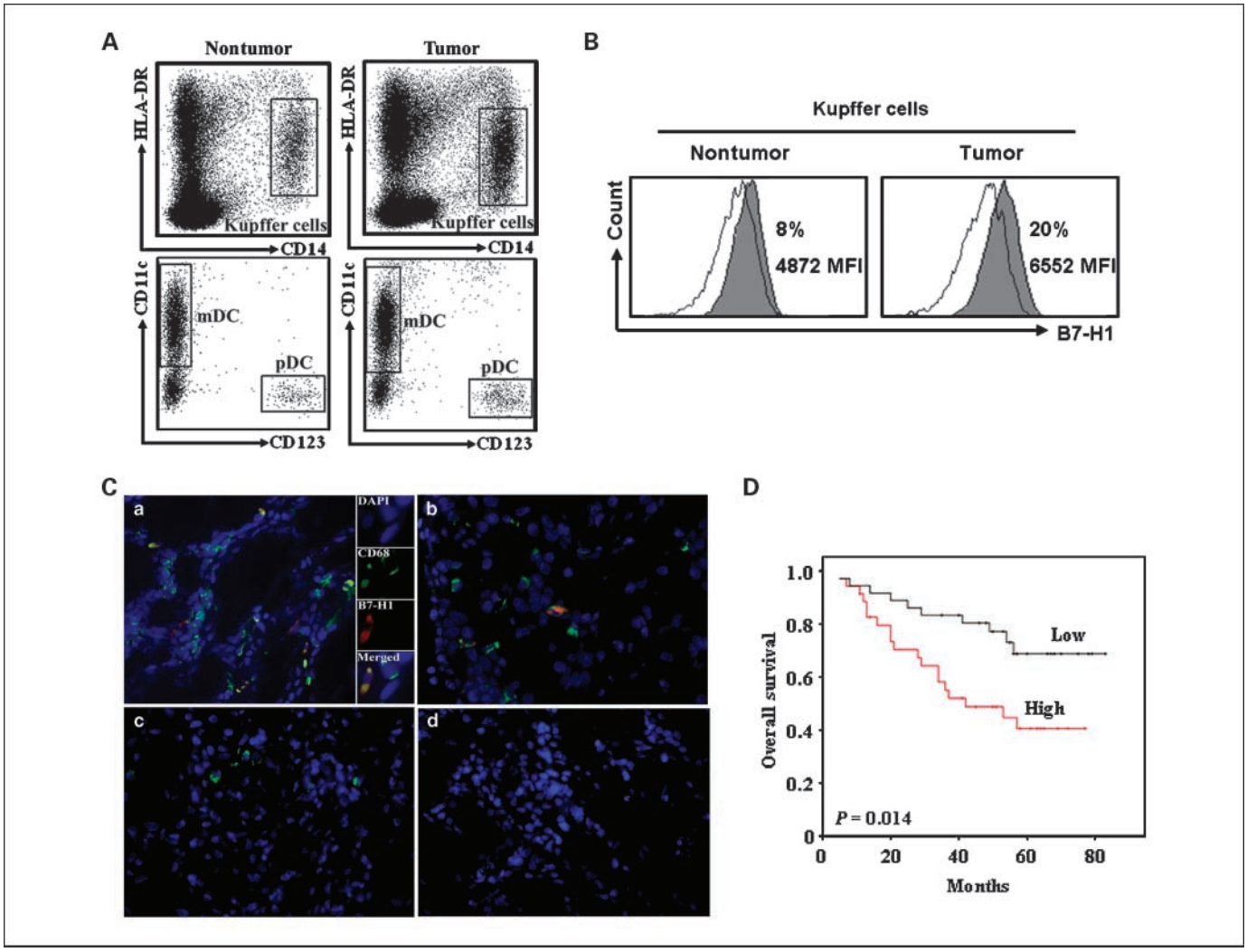

Figure 1. KCs express increased B7-H1 in human HCC. APC subsets in human HCC were analyzed by FACS. *A,* CD45$^+$ leukocytes were analyzed and gated on Lin$^-$HLA-DR$^+$ cells. Representative dot plots of KCs (HLA-DR$^+$CD14$^+$), pDCs (Lin$^-$HLA-DR$^+$CD4$^+$CD11c$^-$CD123$^+$), and mDCs (Lin$^-$HLA-DR$^+$CD4$^+$CD11c$^+$CD123$^-$) from both tumor tissues or nontumor tissues. *B,* representative FACS histogram of B7-H1$^+$ KCs. *Filled histogram,* B7-H1 expression; *open histogram,* antibody isotype control. *C,* B7-H1$^+$KCs in HCC tumor tissue (*a*), surrounding nontumor tissue (*b*), and normal liver tissue (*c*). The immunohistochemistry showed that B7-H1 (*red*) staining was found on CD68$^+$ KCs (*green*) in HCC tumor tissue. *Blue,* nuclear was stained by DAPI. Mouse IgG1 and IgG2b were used as isotype controls (*d*) for B7-H1 and CD68 staining, respectively. Representative sections are shown from eight patients. Magnification, ×400. *D,* Kaplan-Meier survival curves of HCC patients as determined by B7-H1 expression on immunohistochemistry of tumor tissue. *Black line,* low expression (n = 36); *red line,* high expression (n = 35). P = 0.014.

Downloaded from http://aacrjournals.org/cancerres/article-pdf/69/20/8067/2615403/8067.pdf by guest on 01 December 2023

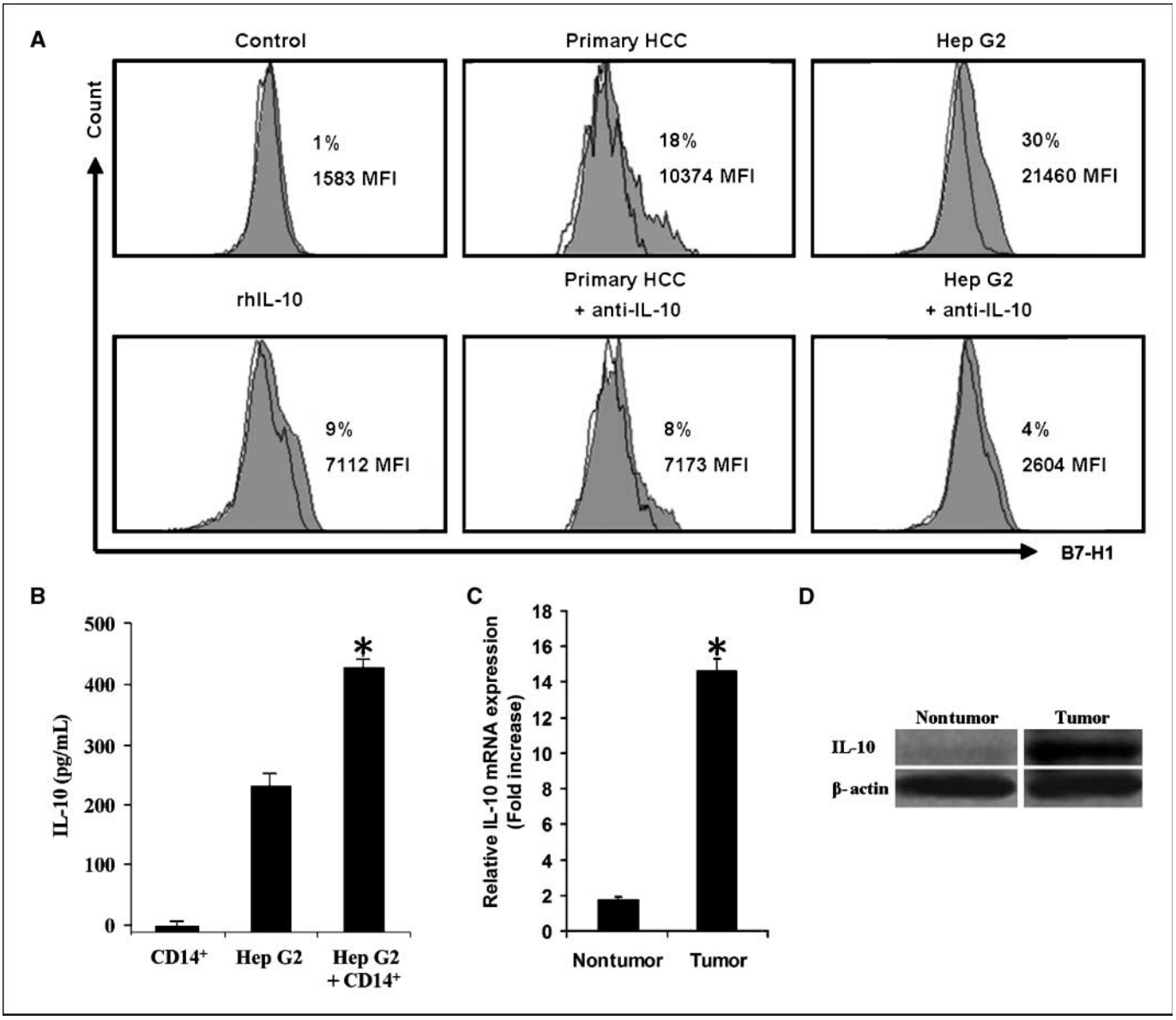

Figure 2. HCC microenvironmental factors induce monocyte B7-H1 expression. $CD14^+$ monocytes from healthy donor blood were sorted and cocultured with primary HCC tumor cells or Hep G2 cells in a Transwell system for 48 h. B7-H1 expression on monocytes was determined by FACS. *A,* $CD14^+$ monocytes cocultured with primary HCC tumor cells or Hep G2 cells expressed more B7-H1 than $CD14^+$ cells alone (control). B7-H1 expression increased moderately on monocytes alone with recombinant human IL-10 (10 ng/mL). Coculture treatment with anti–IL-10 neutralizing antibody inhibited B7-H1 expression. Data are representative of five independent experiments for Hep G2 and triplicate cultures for primary HCC. *Filled histogram,* B7-H1 expression; *open histogram,* antibody isotype control. *B,* supernatants were collected from Transwells and IL-10 was detected by ELISA. *Columns,* mean ($n = 5$ experiments); *bars,* SE. *, $P < 0.05$ versus $CD14^+$ monocytes alone or Hep G2 cells alone. *C,* representative Western blot for IL-10 protein in HCC versus nontumor liver tissue ($n = 8$ patients). *D,* real-time RT-PCR for IL-10 expression ($n = 8$ patients). *, $P < 0.05$.

$CD14^+$ cells from blood of healthy donors were used as control of tumor-associated KCs and showed similar results as the $CD8^+$ T-cell alone cultures (data not shown) and were also similar to the mouse anti-human IgG1 isotype control (Fig. 5*D*).

Discussion

An immune-suppressive environment has been previously described in patients with HCC comprising decreased numbers of $CD8^+$ T cells and increased regulatory T cells (3, 25). However, the underlying mechanisms controlling effector function remain poorly defined within human HCC. Furthermore, the nature and significance of B7-H1 and PD-1 in human HCC are likewise incompletely defined. In the current investigation, we have shown that HCC environmental factors stimulate B7-H1 expression on KCs and that the B7-H1/PD-1 pathway contributes to impaired effector T-cell function in the HCC environment.

B7-H1 has been reported to be expressed on multiple APC subsets (7, 8). It has been shown that liver-resident pDCs or mDCs express B7-H1 after transplantation or virus infection (26, 27). We found that in the HCC environment, B7-H1 expression is confined to KCs but is minimally expressed on mDCs, pDCs, or HCC tumor cells. A significant number of $B7\text{-}H1^+$ KCs in HCC tissue were noted compared with surrounding nontumor tissue. Tumor-associated

Downloaded from http://aacrjournals.org/cancerres/article-pdf/69/20/8067/2615403/8067.pdf by guest on 01 December 2023

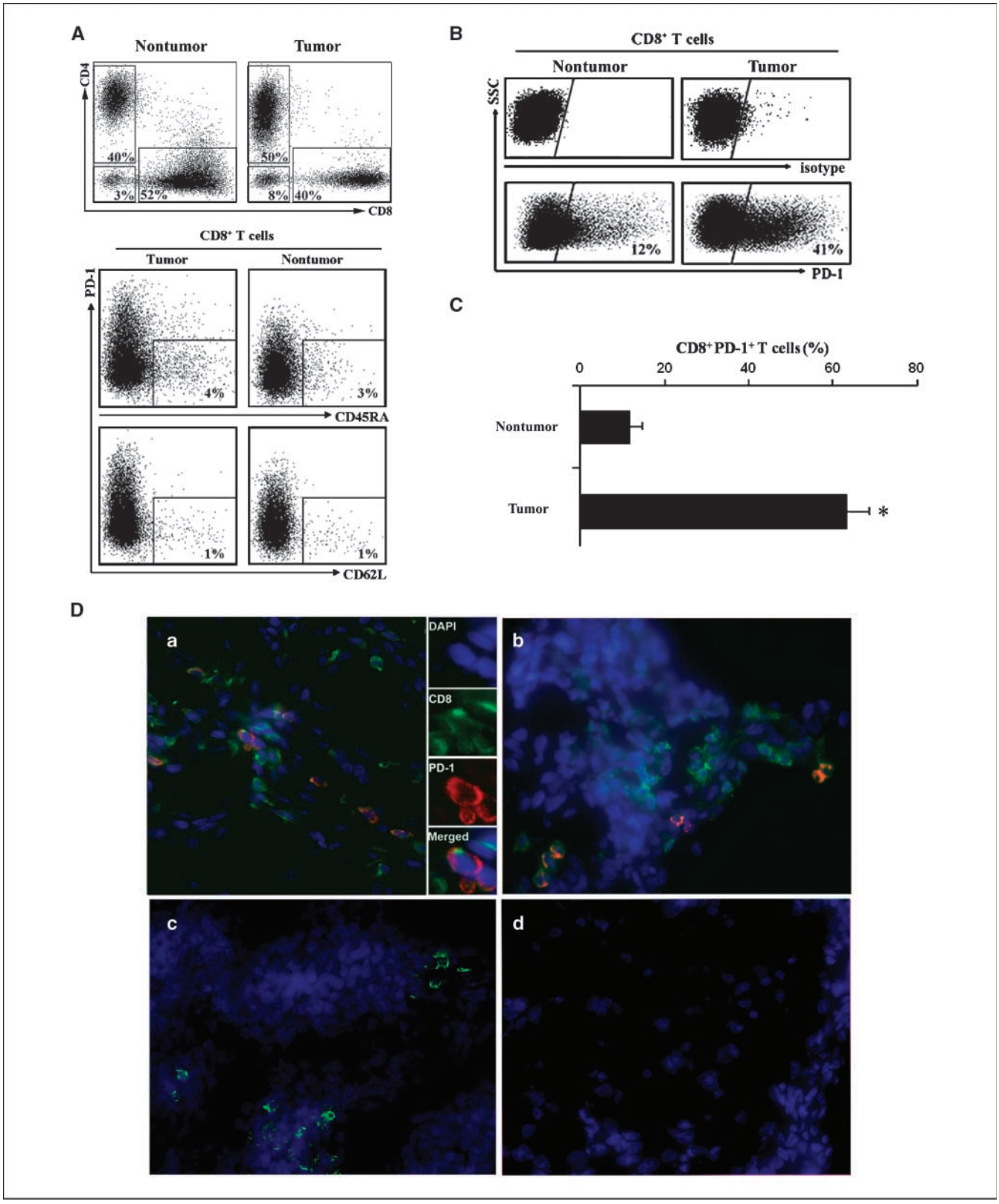

Figure 3. HCC tumor-associated $CD8^+$ T cells highly express PD-1. Human HCC T-cell subsets were analyzed by FACS. *A, top,* representative dot plots of $CD4^+$ and $CD8^+$ T cells from 20 HCC patients gated on $CD3^+$ cells. The proportions of $CD4^+$ and $CD8^+$ T cells in both tumor tissue and nontumor tissue. *Bottom,* representative phenotype dot plots of $CD8^+$ T cells showed both in HCC tumor and nontumor tissues that <5% of $CD8^+$ T cells are $CD45RA^+$ or $CD62L^+$ ($n = 8$ patients). *B,* representative dot plots of $PD\text{-}1^+CD8^+$ T cells from 20 HCC patients in tumor and nontumor tissue. *Top,* isotype control; *bottom,* PD-1 expression on $CD8^+$ cells. *C,* mean percentage of $PD\text{-}1^+CD8^+$ T cells in tumor tissues and nontumor tissues ($n = 20$ patients). *, $P < 0.05$. *D,* $PD\text{-}1^+CD8^+$ T cells in HCC tumor tissue (*a*), surrounding nontumor tissue (*b*), and normal liver tissue (*c*). PD-1 (*red*) staining was largely limited to CD8 cells (*green*). Mouse IgG1 and rat IgG were used as antibody isotype controls (*d*) for PD-1 and CD8 staining, respectively ($n = 8$ patients). *Blue,* DAPI nuclear. Magnification, ×400.

Downloaded from http://aacrjournals.org/cancerres/article-pdf/69/20/8067/2615403/8067.pdf by guest on 01 December 2023

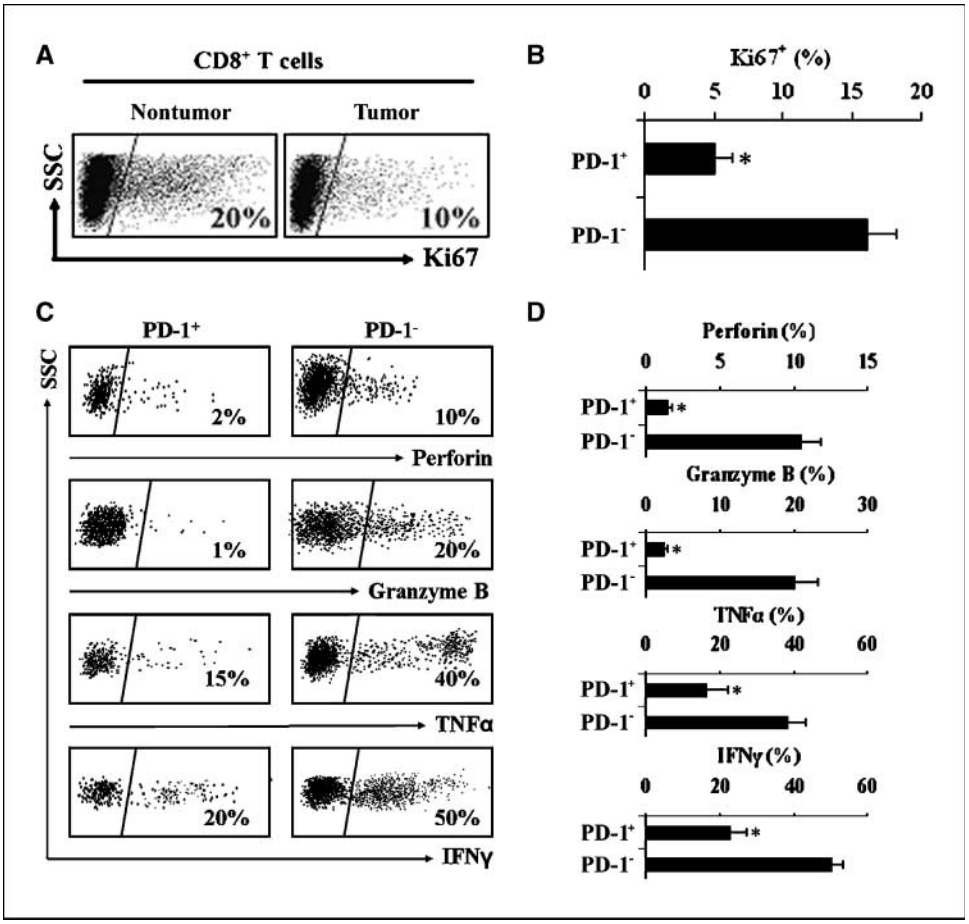

Figure 4. Decreased effector function of PD-1$^+$CD8$^+$ T cells in human HCC. *A,* representative dot plots of Ki67 expression in CD8$^+$ T cells from tumor tissues versus nontumor tissue. *B,* Ki67 expressed as mean percentage cells in PD-1$^+$CD8$^+$ or PD-1$^-$CD8$^+$ T cells in human HCC tissues (n = 20 patients). *, $P < 0.05$. *C,* PD-1$^+$CD8$^+$ T cells in HCC tumor tissues showed decreased effector function compared with PD-1$^-$ T cells. Representative dot plots showing the percentage of perforin-expressing, granzyme B–expressing, TNFα-expressing, and IFNγ-expressing cells in PD-1$^+$ versus PD-1$^-$ CD8$^+$ T cells. *D,* mean percentages of perforin, granzyme B, TNFα, and IFNγ in PD-1$^+$CD8$^+$ T cells in HCC tumor tissues versus PD-1$^-$ T cells (n = 20 patients). *, $P < 0.05$.

IL-10 contributed to B7-H1 up-regulation in the coculture system, and increased IL-10 expression was observed in human HCC. IL-10 expression was elevated in supernatants of monocytes and tumor cells when cocultured. Therefore, both tumor cells and macrophages in the HCC microenvironment could be the source of IL-10 following their interaction with each other. It is also possible that B7-H1 expression could be induced by other tumor-associated cytokines, such as IFNγ and vascular endothelial growth factor (7, 15, 28). Therefore, IL-10 may not the only factor inducing B7-H1 expression in the HCC microenvironment and is consistent with our previous findings in human ovarian carcinoma (15). However, tumor-conditioned KCs are the likely mediator of B7-H1/PD-1 interactions in human HCC.

CD8$^+$ effector T cells mediate antitumor effects directly by expression of either antitumor cytokines (TNFα and IFNγ) or cytotoxic granules (granzyme B and perforin). However, there was no significant difference in the prevalence of CD8$^+$ T-cell distribution and effector phenotype between HCC tissue and surrounding nontumor tissue. Overexpression of PD-1 is a hallmark of exhausted T cells in chronic hepatitis (12, 29). We showed in HCC tissue that higher percentages of CD8$^+$ T cells express PD-1. These PD-1$^+$CD8$^+$ T cells were mainly localized in the HCC stroma as opposed to the tumor nests. Several studies reported the importance of PD-1 expression in dampening antiviral CD8$^+$ T-cell responses in human viral hepatitis (8, 9, 26). Our results in HCC are consistent with these previous findings and are important, as chronic hepatitis or cirrhosis is a major risk factor for human HCC (1). We have shown that PD-1$^+$CD8$^+$ T cells in HCC also display impaired effector phenotype, indicating that the quality and function are altered in HCC.

Inhibitory B7-H1/PD-1 interaction can restrict immune responses against self-antigens. This pathway has emerged as a potential therapeutic target for treating cancer (13–16). In this study, we show that CD8$^+$ T cells and KCs in human HCC tumor tissues expressed high levels of PD-1 and B7-H1, respectively, whereas other molecules (i.e., CD80 and B7-DC) were not detected. Exhausted CD8$^+$ cells were able to be rescued following B7-H1 or PD-1 blockade using monoclonal antibodies, resulting in improved effector responses following TCR stimulation and stimulation with tumor-specific antigens. We have previously shown a role for B7-H1 to inhibit tumor immune responses in human ovarian carcinoma (15). Other investigators have observed that blocking B7-H1/PD-1 enhances the function of antigen-specific T cells in infectious diseases (12, 28, 30, 31).

To our knowledge, this is the first evidence that B7-H1$^+$ APCs and PD-1$^+$ T cells are physically localized in the same site of

Downloaded from http://aacrjournals.org/cancerres/article-pdf/69/20/8067/2615403/8067.pdf by guest on 01 December 2023

liver or within HCC and that T-cell effector function could be rescued by blocking B7-H1/PD-1 interactions, providing important therapeutic implications. By overall survival analysis, we observed that elevated B7-H1 expression in HCC is indeed associated with poorer prognosis in HCC patients as has been recently reported by other investigators (32). Altogether, our data suggest that B7-H1/PD-1 interactions mediate immune suppression in human HCC and B7-H1 expression in tumor was associated with clinical outcome. The suppressive interaction between KCs and T cells using B7-H1/PD-1 interactions in HCC

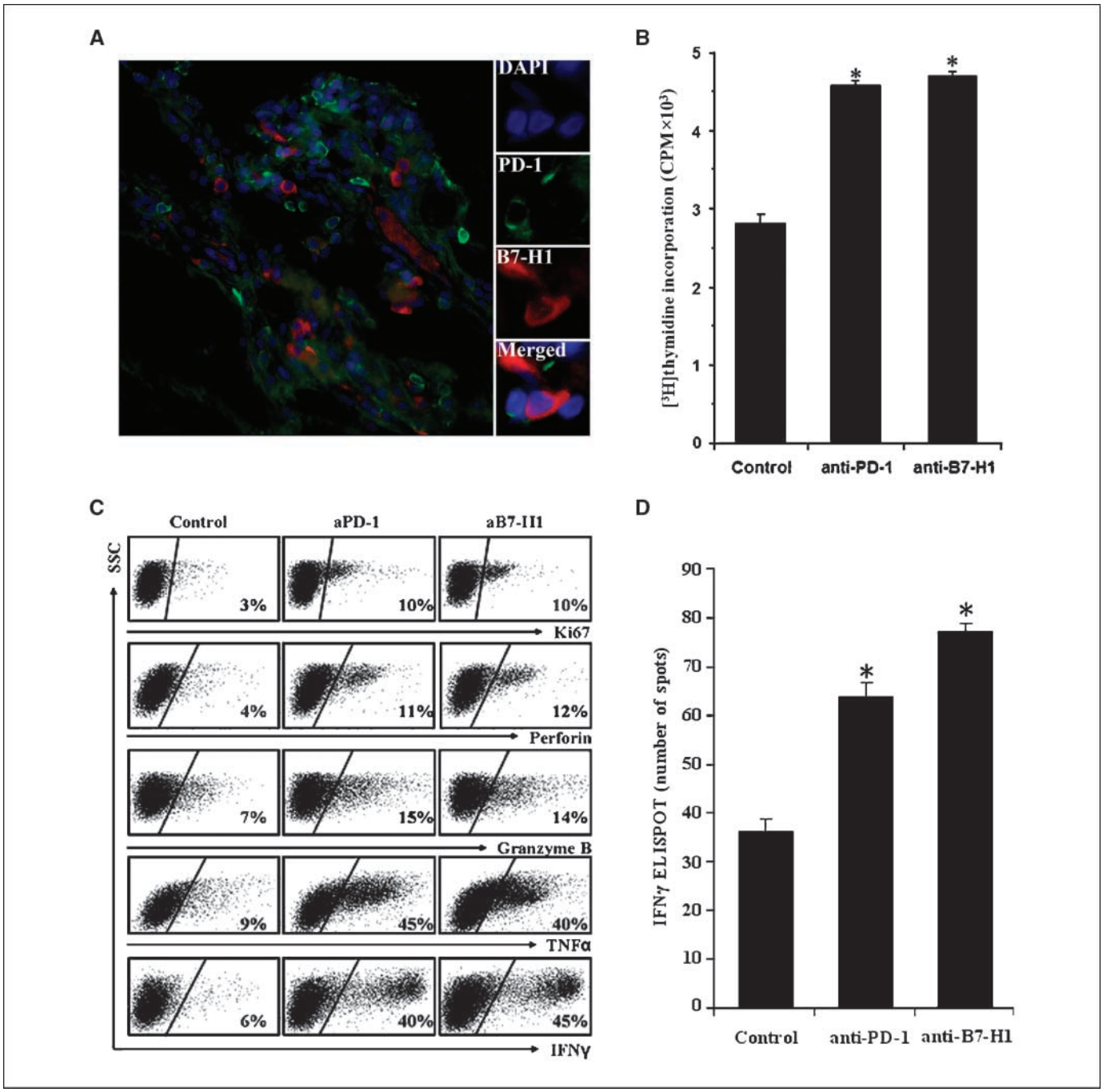

Figure 5. B7-H1$^+$ and PD-1$^+$ cells were colocalized in HCC and mediated T-cell immune suppression. *A,* PD-1$^+$ cells (*green*) were colocalized with B7-H1$^+$ cells (*red*) and DAPI nuclear staining (*blue*). Magnification, ×400. Representative data for eight patients. *B* and *C,* blocking B7-H1 or PD-1 increased T-cell effector function. CD14$^+$ and CD8$^+$ cells were sorted from human HCC and cocultured for 5 d with anti-CD3 and anti-CD28 antibodies. Where indicated, anti–PD-1 or anti–B7-H1 monoclonal antibodies were added and compared with control (mouse anti-human IgG1 isotype control for both anti–PD-1 and anti–B7-H1 antibodies). *B,* CD8$^+$ T-cell proliferation was determined by [^{3}H]thymidine incorporation. *Columns,* mean counts per minute (*CPM*) of five experiments; *bars,* SE. *, $P < 0.05$ versus isotype control. *C,* expression of Ki67, perforin, granzyme B, and cytokines was determined by FACS analysis with representative dot plots shown from five experiments. *D,* HCC-specific CD8$^+$ T-cell response. CD8$^+$ T cells were stimulated with KCs loaded with autologous HCC lysates over 5 d and HCC-specific IFNγ was determined by ELISPOT in the presence or absence of anti–B7-H1 or anti–PD-1 antibody ($n = 3$ experiments). *Columns,* mean number of IFNγ spots per 10^5 CD8$^+$ T cells; *bars,* SE. *, $P < 0.05$ versus isotype control.

Downloaded from http://aacrjournals.org/cancerres/article-pdf/69/20/8067/2615403/8067.pdf by guest on 01 December 2023

patients suggests that targeted therapies against this pathway represent a promising approach to enhance T-cell immunity to human HCC.

Disclosure of Potential Conflicts of Interest

No potential conflicts of interest were disclosed.

Acknowledgments

Received 3/11/09; revised 7/22/09; accepted 8/4/09; published OnlineFirst 10/13/09.

Grant support: Tissue Procurement Core of the University of Michigan Comprehensive Cancer Center grant CA46952.

The costs of publication of this article were defrayed in part by the payment of page charges. This article must therefore be hereby marked *advertisement* in accordance with 18 U.S.C. Section 1734 solely to indicate this fact.

We thank Dr. Li Dong Wang (University of Michigan Medical Center) for the Western blot analysis.

References

1. El-Serag HB, Marrero JA, Rudolph L, et al. Diagnosis and treatment of hepatocellular carcinoma. Gastroenterology 2008;134:1752–63.
2. Zou W. Immunosuppressive networks in the tumour environment and their therapeutic relevance. Nat Rev Cancer 2005;5:263–74.
3. Gao Q, Qiu SJ, Fan J, et al. Intratumoral balance of regulatory and cytotoxic T cells is associated with prognosis of hepatocellular carcinoma after resection. J Clin Oncol 2007;25:2586–93.
4. Ossendorp F, Mengedé E, Camps M, et al. Specific T helper cell requirement for optimal induction of cytotoxic T lymphocytes against major histocompatibility complex class II negative tumors. J Exp Med 1998;187:693–702.
5. Gajewski TF, Meng Y, Blank C, et al. Immune resistance orchestrated by the tumor microenvironment. Immunol Rev 2006;213:131–45.
6. Keir ME, Butte MJ, Freeman GJ, et al. PD-1 and its ligands in tolerance and immunity. Annu Rev Immunol 2008;26:677–704.
7. Zou W, Chen L. Inhibitory B7-family molecules in the tumour microenvironment. Nat Rev Immunol 2008;8:467–477.
8. Yamazaki T, Akiba H, Iwai H, et al. Expression of programmed death 1 ligands by murine T cells and APC. J Immunol 2002;169:5538–45.
9. Azuma T, Yao S, Zhu G, et al. B7-H1 is a ubiquitous antiapoptotic receptor on cancer cells. Blood 2008;111:3635–43.
10. Wang S, Bajorath J, Flies DB, et al. Molecular modeling and functional mapping of B7-H1 and B7-DC uncouple costimulatory function from PD-1 interaction. J Exp Med 2003;197:1083–91.
11. Evans A, Riva A, Cooksley H, et al. Programmed death 1 expression during antiviral treatment of chronic hepatitis B: impact of hepatitis B e-antigen seroconversion. Hepatology 2008;48:759–69.
12. Nakamoto N, Kaplan DE, Coleclough J, et al. Functional restoration of HCV-specific CD8 T cells by PD-1 blockade is defined by PD-1 expression and compartmentalization. Gastroenterology 2008;134:1927–37, 1937.e1–2.
13. Dong H, Strome SE, Salomao DR, et al. Tumor-associated B7-H1 promotes T-cell apoptosis: a potential mechanism of immune evasion. Nat Med 2002;8:793–800.
14. Curiel TJ, Wei S, Dong H, et al. Blockade of B7-H1 improves myeloid dendritic cell-mediated antitumor immunity. Nat Med 2003;9:562–7.
15. Strome SE, Dong H, Tamura H, et al. B7-H1 blockade augments adoptive T-cell immunotherapy for squamous cell carcinoma. Cancer Res 2003;63:6501–5.
16. Yamamoto R, Nishikori M, Kitawaki T, et al. PD-1-PD-1 ligand interaction contributes to immunosuppressive microenvironment of Hodgkin lymphoma. Blood 2008;111:3220–4.
17. Crispe IN, Giannandrea M, Klein I, et al. Cellular and molecular mechanisms of liver tolerance. Immunol Rev 2006;213:101–18.
18. Dong H, Zhu G, Tamada K, et al. B7-H1 determines accumulation and deletion of intrahepatic $CD8^+$ T lymphocytes. Immunity 2004;20:327–36.
19. Iwai Y, Terawaki S, Ikegawa M, et al. PD-1 inhibits antiviral immunity at the effector phase in the liver. J Exp Med 2003;198:39–50.
20. Kryczek I, Liu R, Wang G, et al. FOXP3 defines regulatory T cells in human tumor and autoimmune disease. Cancer Res 2009;69:3995–4000.
21. Wang L, Heidt DG, Lee CJ, et al. Oncogenic function of ATDC in pancreatic cancer through Wnt pathway activation and β-catenin stabilization. Cancer Cell 2009;15:207–19.
22. Miura Y, Nishimura Y, Katsuyama H, et al. Involvement of IL-10 and Bcl-2 in resistance against an asbestos-induced apoptosis of T cells. Apoptosis 2006;11:1825–35.
23. Sindić A, Hirsch JR, Velic A, et al. Guanylin and uroguanylin regulate electrolyte transport in isolated human cortical collecting ducts. Kidney Int 2005;67:1420–7.
24. Butte MJ, Keir ME, Phamduy TB, et al. Programmed death-1 ligand 1 interacts specifically with the B7-H1 costimulatory molecule to inhibit T cell responses. Immunity 2007;27:111–22.
25. Fu J, Xu D, Liu Z, et al. Increased regulatory T cells correlate with CD8 T-cell impairment and poor survival in hepatocellular carcinoma patients. Gastroenterology 2007;132:2328–39.
26. Tokita D, Mazariegos GV, Zahorchak AF, et al. High PD-L1/CD86 ratio on plasmacytoid dendritic cells correlates with elevated T-regulatory cells in liver transplant tolerance. Transplantation 2008;85:369–77.
27. Chen L, Zhang Z, Chen W, et al. B7-H1 up-regulation on myeloid dendritic cells significantly suppresses T cell immune function in patients with chronic hepatitis B. J Immunol 2007;178:6634–41.
28. Lee SJ, Jang BC, Lee SW, et al. Interferon regulatory factor-1 is prerequisite to the constitutive expression and IFN-γ-induced upregulation of B7-H1 (CD274). FEBS Lett 2006;580:755–62.
29. Zhang Z, Zhang JY, Wherry EJ, et al. Dynamic programmed death 1 expression by virus-specific CD8 T cells correlates with the outcome of acute hepatitis B. Gastroenterology 2008;134:1938–49, 1949.e1–3.
30. Day CL, Kaufmann DE, Kiepiela P, et al. PD-1 expression on HIV-specific T cells is associated with T-cell exhaustion and disease progression. Nature 2006;443:350–4.
31. Velu V, Titanji K, Zhu B, et al. Enhancing SIV-specific immunity *in vivo* by PD-1 blockade. Nature 2009;458:206–10.
32. Gao Q, Wang XY, Qiu SJ, et al. Overexpression of PD-L1 significantly associates with tumor aggressiveness and postoperative recurrence in human hepatocellular carcinoma. Clin Cancer Res 2009;15:971–9.

Downloaded from http://aacrjournals.org/cancerres/article-pdf/69/20/8067/2615403/8067.pdf by guest on 01 December 2023